

Evaluation of White Matter Microstructural Alterations in Patients with Post-Stroke Cognitive Impairment at the Sub-Acute Stage

Chunxue He^{1,2,*}, Mingqiang Gong^{3,4,*}, Gengxiao Li^{1,2}, Yunxia Shen², Longyin Han⁵, Bin Han⁶, Mingwu Lou²

¹Shenzhen Clinical Medical College, Guangzhou University of Chinese Medicine, Shenzhen, People's Republic of China; ²Department of Radiology, Longgang District Central Hospital of Shenzhen, Shenzhen, People's Republic of China; ³The Fourth Clinical Medical College of Guangzhou University of Chinese Medicine, Shenzhen, People's Republic of China; ⁴Department of Acupuncture, Shenzhen Traditional Chinese Medicine Hospital, Shenzhen, People's Republic of China; ⁵Department of Neurology, Beijing Longfu Hospital, Beijing, People's Republic of China; ⁶Department of Rehabilitation Medicine, Longgang District Central Hospital of Shenzhen, Guangdong, People's Republic of China

*These authors contributed equally to this work

Correspondence: Bin Han; Mingwu Lou, Tel +86 13928488998; +86 13808854650, Email hbbb08@163.com; mingwulou@sina.com

Purpose: To investigate white matter alterations in post-stroke cognitive impairment (PSCI) patients at the subacute stage employing diffusion kurtosis and tensor imaging.

Methods: Thirty PSCI patients at the subacute phase and 30 healthy controls (HC) underwent diffusion kurtosis imaging (DKI) scans and neuropsychological assessments. Based on the tract-based spatial statistics and atlas-based ROI analysis, fractional anisotropy (FA), mean diffusivity (MD), mean kurtosis (MK), kurtosis fractional anisotropy (KFA), axial kurtosis (AK), and radial kurtosis (RK) were compared in specific white matter fiber bundles between the groups (with family-wise error correction). Adjusting for age and gender, a partial correlation was conducted between neurocognitive assessments and DKI metrics in the PSCI group.

Results: In comparison with the HC, PSCI patients significantly showed decreased MK, RK, and FA and increased MD values in the genu of corpus callosum, anterior limb internal capsule, and left superior corona radiata. In addition, DKI detected more white matter region changes in MK (31/48), KFA (40/48), and RK (25/48) than DTI with FA (28/48) and MD (21/48), which primarily consisted of the right cingulum, right superior longitudinal fasciculus, and left posterior limb of internal capsule. In the left anterior limb of internal capsule, MK and RK values were significantly negatively correlated with TMT-B ($r = -0.435$ and -0.414 , $P < 0.05$), and KFA values ($r = -0.385$, $P < 0.05$) of corpus callosum negatively associated with TMT-B.

Conclusion: Combining DTI, DKI, and neuropsychological tests, we found extensive damaged white matter microstructure and poor execution performance in subacute PSCI patients. DKI could detect more subtle white matter changes than DTI metrics. Our findings provide added information for exploring the mechanisms of PSCI and conducting cognitive rehabilitation in the subacute stage.

Keywords: diffusion kurtosis imaging, diffusion tensor imaging, subacute ischemic stroke, cognitive impairment

Introduction

Cognitive impairment is a common complication of stroke. Although a frequent consequence, it is often not paid much attention as motor and sensory deficit.¹ The prevalence of post-stroke cognitive impairment (PSCI) ranges from 20% to 80%.² About 37% of patients with lacunar stroke suffer complications of mild cognitive impairment or dementia.³ According to a previous study, the prevalence of post-stroke dementia within one month of suffering a stroke was 20.4%, and the frequency of dementia-related lacunar infarction was seven times higher than that in intracerebral hemorrhage.⁴ There, early assessment of cognitive impairment in patients with ischemic stroke is of great significance in the clinical setting. Subacute ischemic infarction generally occurs within one month of a stroke event.^{5,6} Clinical observation during the subacute phase of ischemic stroke can predict the likelihood of cognitive recovery six months post-stroke.⁷ Therefore,

this phase may provide an early opportunity for the appraisal of cognitive status and brain structural changes after ischemic stroke.

To date, the mechanism underlying cognitive decline in patients with subacute ischemic stroke remains poorly understood. Remarkably, neuroimaging techniques have contributed to the study of disease characteristics in patients with PSCI. The conventional magnetic resonance imaging (MRI) technique is valuable for evaluating the extent and location of ischemic stroke. However, it cannot provide information about the microstructural integrity of white matter, especially in normal-appearing white matter as shown by the fluid-attenuated inversion recovery (FLAIR) sequence. Diffusion tensor imaging (DTI), as a non-invasive MRI technique, has been widely used to detect white matter microstructural integrity that are not distinguished on conventional MRI. Water diffusion, which is sensitive to tissue microstructure, provides a method for investigating neural fiber integrity. Anisotropic water diffusion in white matter is the basis for DTI in tracking fiber pathways.⁸ The displacement of water molecules and degree of fiber coherence or directionality can be estimated from DTI-derived metrics, such as fractional anisotropy (FA) and mean diffusivity (MD).⁹ According to animal models of DTI, a decrease in FA and an increase in MD reflects alterations in white matter integrity that may be correlated to the disorganization and loss of axonal membranes and myelin sheaths.¹⁰ Decreased FA and increased MD values have been reported in patients with acute PSCI and mild cognitive impairment (MCI).^{11,12} Furthermore, MD values of the hippocampus were superior to volume measurements and functional connectivity in identifying patients with early MCI.¹³

Diffusion kurtosis imaging (DKI) is an extension of DTI, which provides a more complete characterization of tissue structure by quantifying the non-Gaussian degree of water diffusion.¹⁴ The DKI model-derived metrics consist of mean kurtosis (MK), axial kurtosis (AK), radial kurtosis (RK), and kurtosis fractional anisotropy (KFA), which estimate the degree of diffusional non-Gaussianity.¹⁵ To investigate the complexity of white matter, DKI has been used in vascular cognitive impairment.^{16,17} However, these studies merely observed regions of the medial temporal cortex and cingulate gyrus. To the best of our knowledge, few studies have focused on white matter profiles of cognitive dysfunction with ischemic stroke at the subacute stage. This study sought to (i) evaluate whole-brain white matter changes by means of tract-based spatial statistics (TBSS) and atlas-based region of interest (ROI) analysis in patients with PSCI during the subacute phase, (ii) detect whether DKI metrics provide more diffusion profiles on white matter microstructural discrepancy than DTI, and (iii) analyze the underlying association between the microstructural changes of specific tracts and neurocognitive assessments.

Materials and Methods

Participants

With the approval of the Ethics Committee of the Longgang District Central Hospital of Shenzhen (2019ECPJ013), 30 patients with PSCI were enrolled in this prospective study. Inclusion criteria were (1) participant's age of 40–65 years, (2) hospitalization with an ischemic stroke event within one month (determined by MRI scans and lesion ≤ 15 mm in diameter), (3) Montreal Cognitive Assessment (MoCA) < 26 points, National Institute of Health Stroke Scale (NIHSS) < 7 points, and dependence in function (modified Rankin Score [mRS] ≤ 3 points), and (4) right-hand dominance. The exclusion criteria included (1) brain lesions other than ischemic cerebral infarction; (2) inability to perform neuropsychological tests or contraindication to MRI; (3) history of pre-stroke dementia, AD, Parkinson's disease, and head trauma; (4) moderate-severe white matter hyperintensity (the Fazekas score of 3–6);¹⁸ (5) depressive disorder (the 17-Item of the Hamilton Rating Scale for Depression > 7).¹⁹ Thirty healthy controls (HC) matched with patients according to age, gender, and education were recruited. All participants provided written informed consent. This study was conducted in accordance with the Declaration of Helsinki.

Clinical Assessment

All participants underwent neuropsychological assessments, including the MoCA, Trail Making Test, parts A (TMT-A) and B (TMT-B), and 30-item Boston Naming Test (BNT). The MoCA was used to assess global cognitive functions covering visual-spatial structure skills, executive function, naming, memory, attention, calculation, language, abstraction,

and orientation. A MoCA score <26 points indicated cognitive impairment (1 point was added when years of education <12). TMT can assess multiple executive functions, mainly comprising processing speed, set-shifting, and visuospatial ability.²⁰ BNT reflected the processing and fluency of language in participants. NIHSS and mRS were used to evaluate stroke severity and functional outcome in patients with cognitive dysfunction.²¹

Image Acquisition

MRI data were acquired using a 3.0 T MRI scanner (Siemens Prisma, Germany) equipped with a 64-channel head coil. Axial T2-weighted images were obtained initially with the FLAIR sequence (TR/TE = 9000/95ms, FOV = 220mm×220mm, voxel size = 0.5 mm×0.5 mm×5.0mm, number of slices = 20). The sagittal T1-weighted three-dimensional high-resolution brain anatomical images were obtained with magnetization-prepared rapid acquisition gradient-echo sequence (MPRAGE, TR/TE = 2300/2.32ms, FOV = 240mm×240mm, number of slices = 208). DKI images were obtained with 3 b-values (b = 0, 1000, and 2000s/mm²) along 30 diffusion gradient directions for each non-zero b value using EPI sequence. The parameters were as follows: TR/TE = 7800/73 ms; FOV = 240mm×240 mm; voxel size = 2.0mm×2.0mm×2.0mm; number of slices = 70; and scan time = 8 min, 58s.

Diffusion Data Processing

Global brain volumes were measured with the T1-3D sequence using the Statistical Parametric Mapping software (SPM 12, <http://www.fil.ion.ucl.ac.uk/spm>). The DKI images were processed with FMRIB Software Library (FSL 5.0, <http://www.fmrib.ox.ac.uk/fsl>).²² DKI data pre-processing comprised data format conversion, motion correction, eddy current correction, and non-brain tissue removal. Post-processing was performed with a Diffusional Kurtosis Estimator software package (<http://nitrc.org/projects/dke>).²³ MK, KFA, AK, and RK maps were derived by fitting the diffusion MRI signal measurements to the DKI signal model, with a constrained weighted linear least-squares fitting algorithm by all three b values. Concurrently, DTI parameters (FA and MD) were calculated using two b values (0 and 1000 s/mm²).

TBSS Analysis

TBSS was applied to further characterize the affected regions in voxel-wise differences of diffusion metrics in FSL.²⁴ The following procedures were performed. (1) Each participant's FA data were aligned into the FMRIB58_FA standard space template by means of nonlinear co-registration tool, (2) The mean FA image and mean FA skeleton were created and then FA data were projected on this skeleton. A threshold of 0.2 was set for the mean FA skeleton to include major white matter bundles but exclude peripheral tracts.

Atlas-Based ROIs Quantitative Analysis

The Johns Hopkins University (JHU) white matter tractography atlas parcel white matter into 48 ROIs to anatomically localize alterations.²⁵ In the acute and chronic phases of ischemic PSCI, white matter alterations have been observed in the corpus callosum, corona radiata, and bilateral internal capsule.^{26,27} The cingulate gyrus, placed centrally in the Papez circuit, is involved in the regulation of cognition,²⁸ and associations have been delineated between the superior longitudinal fasciculus and memory.^{29,30} Therefore, the right cingulum (cingulate gyrus), internal capsule (bilateral anterior limb and left posterior limb), corpus callosum, right superior longitudinal fasciculus, and left superior corona radiata were located and labeled using JHU-ICBM-DTI-81 (<http://cmrm.med.jhmi.edu>) (Figure 1). Corresponding FA, MD, MK, KFA, AK, and RK values were quantified accordingly.

Statistical Analysis

Statistical analysis was performed with SPSS version 26.0 software. The Shapiro Wilk (S-W) test was used for testing the normality distribution of clinical data. The chi-square test was used for calculating type variables. To test differences between two group variables, the independent sample *t*-test for normally distributed data and Mann Whitney *U*-test for non-normally distributed data were performed respectively. To directly compare cognitive functions in different domains, the raw test results of TMT-A, TMT-B, and BNT were transformed into z-scores. Partial correlation was applied to explore the association between ROI-based DKI values in specific fiber tracts and scores of various cognitive

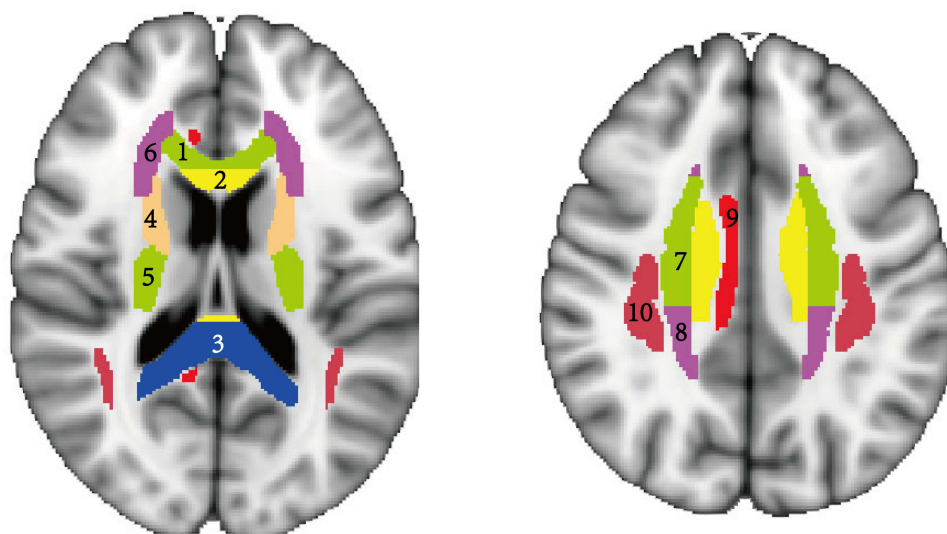


Figure 1 Selected ROIs based on the JHU-ICBM-Labels-1mm template.

Notes: 1–3, genu/body/splenium of the corpus callosum; 4–5, anterior/ posterior limb of internal capsule; 6–8, anterior/ superior/ posterior corona radiata; 9, Cingulum (hippocampus); 10, superior longitudinal fasciculus.

assessments, including MoCA, TMT-A, TMT-B, and BNT, after adjusting for age and gender. For TBSS, non-parametric permutation tests were performed by randomize order (5000 permutations) to determine the between-group discrepancy, and the statistical maps were processed at the cluster-level with threshold-free cluster enhancement (TFCE). $P < 0.05$, corrected for family-wise error (FWE), was considered statistically significant.

Results

Demographics and Clinical Measurements

Sixty participants were enrolled after excluding patients with poor imaging quality and incomplete clinical information. Demographic and clinical data are shown in Table 1. No differences were found in age, gender, duration of education, and vascular risk factors (hypertension, diabetes mellitus, hyperlipidemia, and smoking) between the PSCI and HC groups. The groups did not significantly differ in gray matter, white matter, and cerebrospinal fluid volumes ($P > 0.05$). The PSCI group had lower scores in MoCA, TMT-A and B, and BNT than those of the HC ($P < 0.05$, Table 2).

Whole-Brain White Matter Changes and Atlas-Based ROI Analysis

The whole-brain TBSS analysis revealed significantly lower FA, MK, KFA, AK, and RK, and higher MD values in patients with PSCI than the HC ($P < 0.05$, with FWE correction, Figure 2). In the entire 48 white matter ROIs, more white matter fiber tracts had decreased MK (31/48), KFA (40/48), and RK (25/48) than decreased FA (28/48) and increased MD (21/48) in the PSCI group (Table 3). Based on atlas-based ROI analysis, decreased MK, KFA, AK, RK and FA values, and increased MD were mainly observed in the genu of corpus callosum, bilateral anterior limb internal capsule, and left superior corona radiata of the PSCI group ($P < 0.05$, Figure 3A–F). In addition, differences were detected in DKI parameters (MK, RK, and AK values) within the right cingulum (cingulate gyrus), right superior longitudinal fasciculus, and left posterior limb of internal capsule ($P < 0.05$, Figure 3C–F). However, no significant FA and MD differences were found in PSCI patients, when compared with the HC group ($P > 0.05$, Figure 3A and B).

Correlation Between DKI Metrics and Neuropsychological Assessments

After adjusting the age and gender, a partial correlation was found between KFA values and TMT-B in the genu of corpus callosum ($r = -0.385$, $P < 0.05$; Figure 4A). Additionally, negative correlations were observed between MK and RK values of the left anterior limb of internal capsule and the TMT-B ($r = -0.435$ and -0.414 , $P < 0.05$; Figure 4B and C) in the PSCI group.

Table 1 Clinical Characteristics of the PSCI and HC Groups

| Variables | PSCI (n=30) | HC (n=30) | t/ χ^2 Value | P value |
|--|-------------|------------|-------------------|-------------------|
| Demographic characteristics | | | | |
| Age (year) | 56.3 ± 5.8 | 52.3 ± 4.9 | -1.88 | 0.065 |
| Gender (male: female) | 24:6 | 21:9 | 0.80 | 0.37 [#] |
| Education (year) | 7.3±3.3 | 7.9±4.4 | 0.65 | 0.52 |
| Vascular risk factors | | | | |
| Hypertension | 25 (83.3%) | 23 (76.7%) | 0.42 | 0.52 [#] |
| Diabetes mellitus | 12 (40%) | 9 (30%) | 0.66 | 0.42 [#] |
| Hyperlipidemia | 15 (50%) | 12 (40.0%) | 0.61 | 0.44 [#] |
| Smoking | 19 (63.3%) | 17 (56.7%) | 0.28 | 0.60 [#] |
| Clinical scores | | | | |
| NIHSS | 3.8 ± 1.7 | - | - | - |
| mRS | 2.3 ± 0.9 | - | - | - |
| Stroke location | | | | |
| Basal ganglia | 13 | - | - | - |
| Thalamus | 9 | - | - | - |
| Pons | 8 | - | - | - |
| Gray matter volume (ml ³) | 570.7±41.9 | 588.3±44.1 | 1.56 | 0.13 |
| White matter volume (ml ³) | 496.6±56.1 | 505.9±43.5 | 0.70 | 0.48 |
| CSF volume (ml ³) | 421.2±75.8 | 389.0±47.5 | -1.93 | 0.06 |

Note: p values labeled with superscript sign (#) were obtained using the Pearson's chi-square test (2-sided).

Abbreviations: PSCI, post-stroke cognitive impairment; NIHSS, the National Institute of Health Stroke Scale; mRS, modified Rankin Scale; CSF, cerebrospinal fluid.

Table 2 Neuropsychological Data of PSCI and HC Groups

| Domain | PSCI (n=30) | HC (n=30) | t/ χ^2 Value | P value |
|----------------------------|-------------|------------|-------------------|---------|
| Executive function score/5 | 2.3±1.0 | 3.6±0.8 | 5.61 | <0.001 |
| Naming score/3 | 2.3±0.7 | 2.9±0.3 | 4.29 | <0.001 |
| Memory score/5 | 1.7±1.2 | 3.7±0.8 | 8.03 | <0.001 |
| Attention score/6 | 4.5±1.1 | 5.7±0.5 | 5.30 | <0.001 |
| Language score/3 | 1.6±1.0 | 2.9±0.3 | 6.79 | <0.001 |
| Abstract score/2 | 0.4±0.5 | 1.3±0.5 | 7.09 | <0.001 |
| Orientation score/6 | 5.4±0.7 | 5.8±0.4 | 3.07 | <0.05 |
| Total MoCA score/30 | 18.8±2.5 | 26.6±0.8 | 16.40 | <0.001 |
| TMT-A (second) | 98.2±30.7 | 75.2±21.7 | -3.30 | <0.005 |
| TMT-B (second) | 230.1±78.9 | 138.0±40.0 | -5.59 | <0.001 |
| BNT score/30 | 18.2±2.6 | 22.2±2.3 | 6.14 | <0.001 |

Abbreviations: MoCA, Montreal Cognitive Assessment; TMT, Trail Making Test; BNT, Boston Naming Test.

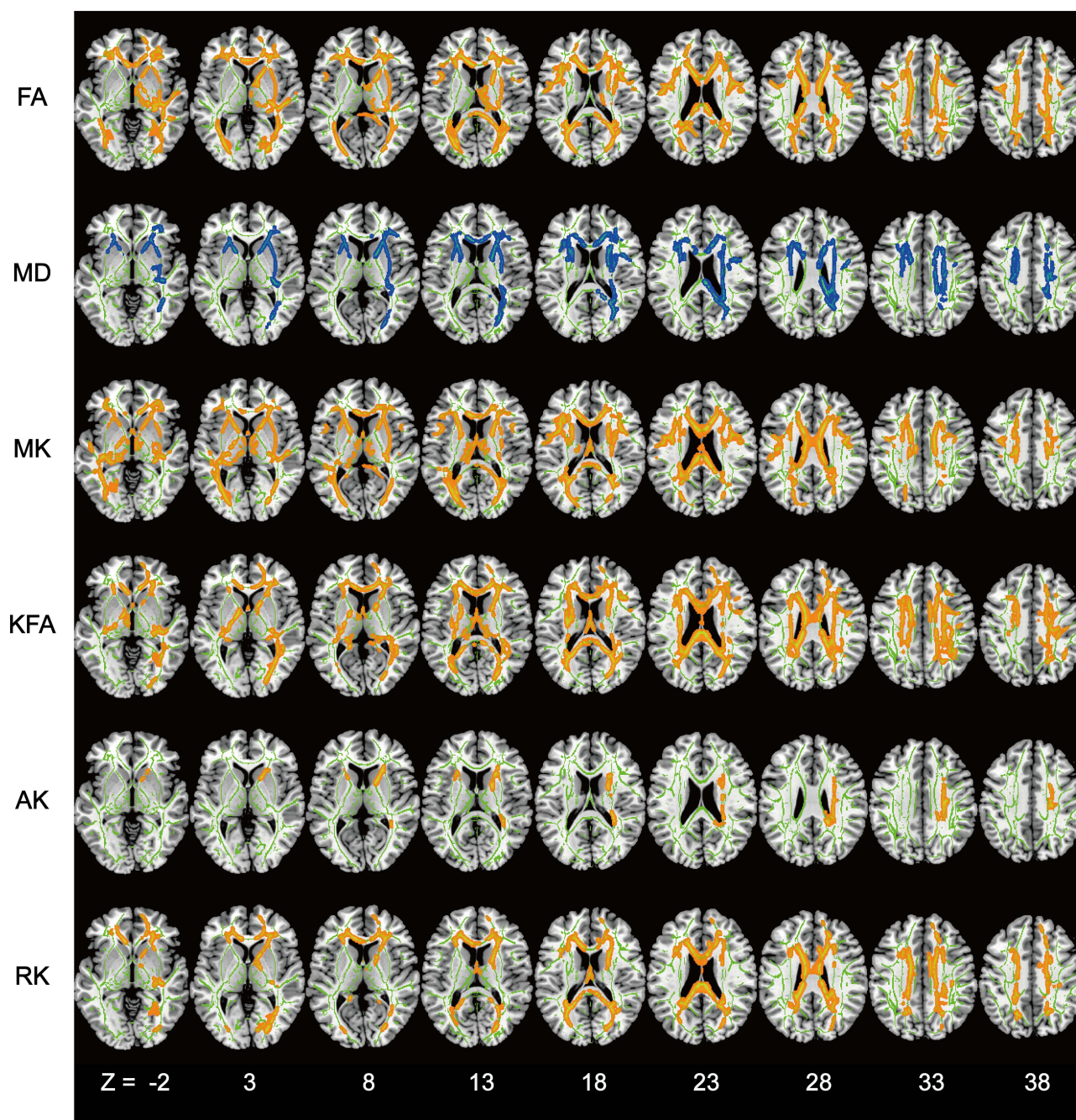


Figure 2 Differences in diffusion tensor metrics and kurtosis metrics between the PSCI and the HC groups.

Notes: The result of contrast is overlaid on the mean FA skeleton (Green) created by TBSS. The blue color represents increased MD values, and orange indicates decreased diffusion parameters in the PSCI group.

Abbreviations: FA, fractional anisotropy; MD, mean diffusivity; MK, mean kurtosis; KFA, kurtosis fractional anisotropy; AK, axial kurtosis; RK, radial kurtosis.

Discussion

In this study, patients with PSCI had loss of white matter integrity in broad white matter regions reflected by the DTI and DKI metrics at the sub-acute stage. Particularly, DKI indices manifested more damaged white matter areas than DTI metrics. Furthermore, a significant association was found between microstructural changes of specific tracts and executive performance. Liu et al¹⁷ found low MK and FA, and high MD values in the cingulate cortex in MCI patients. However, our study differs from the abovementioned study in several ways. First, patients with PSCI at the subacute

Table 3 Diffusion Changes in the White Matter Tracts Between PSCI and HC Groups in the JHU Atlas

| Fiber Tracts | FA | MD | MK | KFA | AK | RK |
|--|-----|-----|-----|-----|-----|-----|
| Corpus callosum | Yes | Yes | Yes | Yes | Yes | Yes |
| Anterior limb of internal capsule | r | b | b | b | b | r |
| Posterior limb of internal capsule | r | r | b | b | r | r |
| Retrolenticular part of internal capsule | r | r | b | b | r | r |
| Anterior corona radiata | b | b | b | b | b | b |
| Superior corona radiata | b | b | b | b | r | b |
| Posterior corona radiata | b | r | b | b | r | b |
| Posterior thalamic radiation | b | r | b | b | r | b |
| External capsule | r | b | b | b | b | r |
| Cingulum (cingulate gyrus) | r | – | r | l | – | r |
| Cingulum (hippocampus) | – | – | – | – | – | – |
| Superior longitudinal fasciculus | b | b | b | b | r | r |
| Superior fronto-occipital-fasciculus | r | b | b | b | r | r |
| Sagittal stratum | – | r | r | l | – | – |
| Uncinate fasciculus | – | – | – | – | – | – |
| Corticospinal tract | – | – | – | l | – | – |
| Cerebral peduncle | r | – | l | b | – | – |
| Inferior cerebellar peduncle | – | – | – | – | – | – |
| Tapetum | – | – | – | – | – | – |
| Medial lemniscus | – | – | – | – | – | – |
| Middle cerebellar peduncle | – | – | – | – | – | – |
| Pontine crossing tract | – | – | – | Yes | – | – |
| Fornix | – | – | Yes | Yes | – | – |

Notes: JHU atlas consists 48 white matter ROIs (left and right). The r, l and b represent fiber tract microstructural changes in the right, left and bilateral side. Yes means damage in the fiber tracts.

Abbreviations: r, right; l, left; b, bilateral.

stage were recruited. Second, whole-brain analysis and ROI-based quantitative analysis were used to compare intergroup differences, which can be beneficial in delineating a comprehensive overview of the microstructural damage. Importantly, disrupted features were characterized by DTI and DKI metrics. Based on the study objectives, DKI was confirmed to be more sensitive in probing white matter alterations, which may be more valuable for identifying high-risk individuals and improving cognitive outcomes following the occurrence of stroke.

The white matter microstructural differences detected by DTI and DKI were found between the PSCI and HC group. The disruption of white matter fibers that interconnect distributed cerebral cortices may be the potential mechanism for cognitive decline.³¹ The corpus callosum, the largest commissural fiber, is a core part of interhemispheric communication and coordination on cognitive performance.³² Notably, it is a vulnerable site for cognitive impairment after acute stroke.³³ The severed corpus callosum markedly reduces interhemispheric functional connectivity between the frontal gyrus and other regions³⁴ involved in executive performance.³⁵ In this study, the PSCI group showed low FA values in the genu of corpus

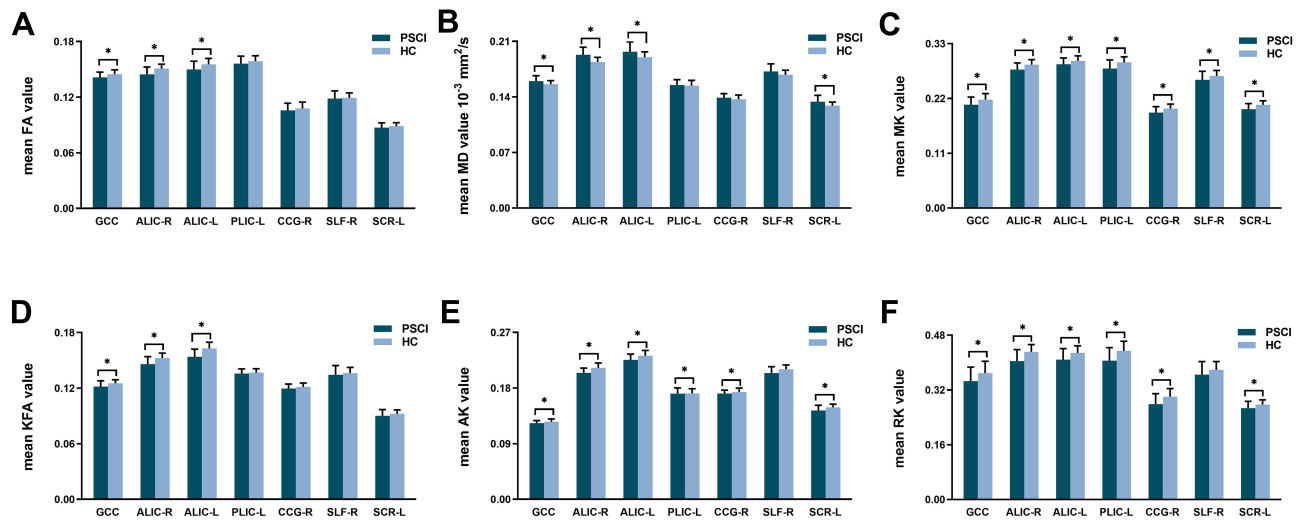


Figure 3 Differences in DTI and DKI metrics for specific fiber tracts between the PSCI and the HC groups.
Notes: *Statistically significant difference ($P < 0.05$). The error bar showed the standard deviation; (A–F) represent the mean FA/ MD/ MK/ KFA/ AK/ RK values of ROIs.
Abbreviations: GCC, genu of corpus callosum; ALIC-R/L, right/left anterior limb of internal capsule; PLIC-L, left posterior limb of internal capsule; CCG-R, right cingulum (cingulate gyrus); SLF-R, right superior longitudinal fasciculus; SCR-L, left superior corona radiata.

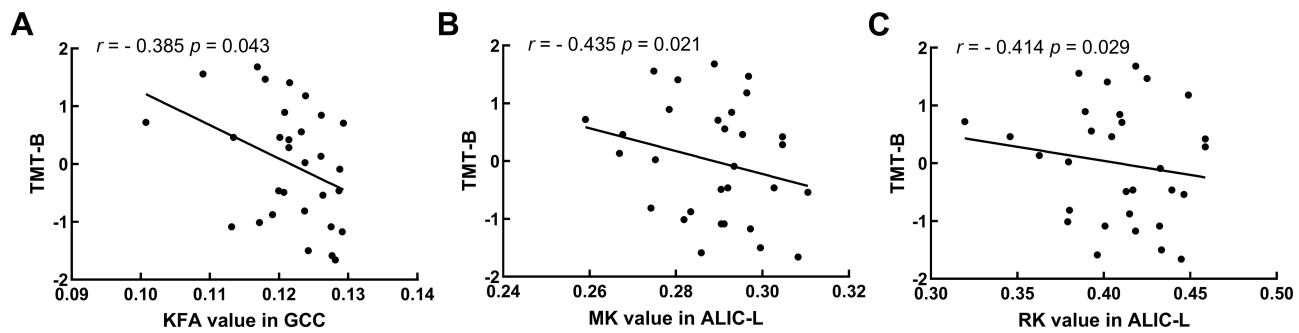


Figure 4 Correlation between DKI values in specific white matter tracts and the neuropsychological test in PSCI group.
Note: (A–C) respectively represent the association between TMT-B and GCC (KFA value) and ALIC-L (MK and RK value).

callosum, with additionally low MK and KFA values. Furthermore, KFA values had a negative correlation with executive function, as determined by TMT-B. Therefore, the damage of the genu of corpus callosum may correlate with executive dysfunction at an early stage of cognitive deterioration. As a part of the limbic-thalamo-cortical circuitry,³⁶ the corona radiata includes thalamic projections and shares the projections at the frontal lobe.²⁵ The disruption of thalamocortical connectivity appears to be a potential pathway for cognitive and sensory dysfunction.^{37–42} Our current study showed that patients with PSCI had decreased MK, AK, RK, and increased MD in the left superior corona radiata. Moreover, differences were more prominent in the bilateral internal capsule in PSCI group than in HC. Importantly, executive performance was found to be associated with decreased MK and RK in the left anterior limb of internal capsule. The anterior limb of internal capsule played a central role in the frontal-subcortical fiber tracts involved in cognitive and limbic circuits.⁴³ Hence, the findings from current and previous studies suggest that the loss of integrity in the internal capsule and corona radiata is likely to be a critical factor for PSCI group at the subacute stage, leading to their poor executive performance.

Diffusion of water molecules in the brain exhibits a non-Gaussian distribution,¹⁵ but the DTI model simplifies water diffusion processes. DKI provides more kurtosis indices for detecting tissue microstructure. Kurtosis refers to a dimensionless measure that is inherent to free or unrestricted diffusion, hence revealing the degree of diffusion restriction.⁴⁴ Furthermore, DKI observations may improve sensitivity and specificity in estimating disease state,⁴⁴ especially

in ischemic tissue characterization.⁴⁵ These features may explain why DKI identified more damaged white matter regions than DTI indices. We observed lower MK, RK and AK values in the cingulum, superior longitudinal fasciculus, and posterior limbs of internal capsule. The cingulum, a bunch of association fiber, interconnects the frontal, parietal, and medial temporal gyri, and primarily engages in the function of memory, execution, and attention.²⁸ The superior longitudinal fasciculus, a bidirectional association tract, plays a role in the communication between the frontal and parietal lobes and regulates executive function, and memory.^{29,46} Reduced MK in the brain is likely related to impoverished cell compartmentalization and an increase in membrane permeability.^{15,47} AK is thought to be primarily affected by intracellular structures, whereas RK is thought to be more influenced by cellular membranes and myelin sheaths.⁴⁵ Cognitive processing relies on the integrity of white matter fibers that interconnect the cerebral cortex. The white matter fiber change in the aforementioned regions manifested reduced tissue complexity, which may be a potential cause of cognitive decline.

This study had some limitations. First, the relatively small number of patients with PSCI may limit the generalizability of our results. However, strict multiple comparison correction (FWE correction) was adopted to increase the robustness of the results. Second, the characteristics of white matter damage in cognitive dysfunction after subacute stroke and relationship between specific tracts and cognitive decline were based on preliminary observations. A longitudinal follow-up is needed to monitor disease progression in future studies.

Conclusion

Patients with PSCI at the subacute stage exhibited extensive white matter microstructural alterations, based on DTI and DKI metrics. More importantly, DKI demonstrated more white matter abnormalities than DTI in regions, such as the cingulum, superior longitudinal fasciculus, and posterior limbs of internal capsule. Moreover, executive dysfunction related to white matter fiber loss was a primary characteristic in patients with subacute PSCI. These findings contribute to our understanding of the mechanism underlying early cognitive decline in PSCI and may improve PSCI rehabilitation.

Acknowledgments

The authors thank all the participants and staff involved in this study. This study was supported by the Traditional Chinese Medicine Bureau of Guangdong Province (No. 20201300) and the Longgang Science Technology and Innovation Commission of Shenzhen (LGKCYLWS2020012).

Author Contributions

All authors made a significant contribution to the work reported, whether that is in the conception, study design, analysis and interpretation; took part in drafting, revising or critically reviewing the article; gave final approval of the version to be published; have agreed on the journal to which the article has been submitted; and agree to be accountable for all aspects of the work.

Disclosure

The authors declare no conflicts of interest in this work.

References

1. Casolla B, Caparros F, Cordonnier C, et al. Biological and imaging predictors of cognitive impairment after stroke: a systematic review. *J Neurol*. 2019;266(11):2593–2604. doi:10.1007/s00415-018-9089-z
2. Sun J, Tan L, Yu J. Post-stroke cognitive impairment: epidemiology, mechanisms and management. *Ann Transl Med*. 2014;2(8):80. doi:10.3978/j.issn.2305-5839.2014.08.05
3. Makin SDJ, Turpin S, Dennis MS, Wardlaw JM. Cognitive impairment after lacunar stroke: systematic review and meta-analysis of incidence, prevalence and comparison with other stroke subtypes. *J Neurol Neurosurg Psychiatry*. 2013;84(8):893–900. doi:10.1136/jnnp-2012-303645
4. Bejot Y, Aboa-Eboule C, Durier J, et al. Prevalence of early dementia after first-ever stroke: a 24-year population-based study. *Stroke*. 2011;42(3):607–612. doi:10.1161/STROKEAHA.110.595553
5. Nys GM, van Zandvoort MJ, van der Worp HB, Kappelle LJ, de Haan EH. Neuropsychological and neuroanatomical correlates of perseverative responses in subacute stroke. *Brain*. 2006;129(Pt 8):2148–2157. doi:10.1093/brain/aw1199

6. Nave AH, Rackoll T, Grittner U, et al. Physical Fitness Training in Patients with Subacute Stroke (PHYS-STROKE): multicentre, randomised controlled, endpoint blinded trial. *BMJ*. 2019;366:15101. doi:10.1136/bmj.15101
7. Vicentini JE, Weiler M, Casseb RF, et al. Subacute functional connectivity correlates with cognitive recovery six months after stroke. *Neuroimage Clin*. 2021;29:102538. doi:10.1016/j.nicl.2020.102538
8. Beaulieu C. The basis of anisotropic water diffusion in the nervous system - a technical review. *NMR Biomed*. 2002;15(7–8):435–455. doi:10.1002/nbm.782
9. Acosta-Cabrero J, Nestor PJ. Diffusion tensor imaging in Alzheimer's disease: insights into the limbic-diencephalic network and methodological considerations. *Front Aging Neurosci*. 2014;6:266. doi:10.3389/fnagi.2014.00266
10. Basser P. Inferring microstructural features and the physiological state of tissues from diffusion-weighted images. *NMR Biomed*. 1995;8:333–344. doi:10.1002/nbm.1940080707
11. Zamboni G, Griffanti L, Jenkinson M, et al. White matter imaging correlates of early cognitive impairment detected by the Montreal cognitive assessment after transient ischemic attack and minor stroke. *Stroke*. 2017;48(6):1539–1547. doi:10.1161/STROKEAHA.116.016044
12. Gyebnár G, Szabó Á, Sirály E, et al. What can DTI tell about early cognitive impairment? - differentiation between MCI subtypes and healthy controls by diffusion tensor imaging. *Psychiatry Res Neuroimaging*. 2018;272:46–57. doi:10.1016/j.psychres.2017.10.007
13. Kliper E, Ben Assayag E, Korczyn AD, et al. Cognitive state following mild stroke: a matter of hippocampal mean diffusivity. *Hippocampus*. 2016;26(2):161–169. doi:10.1002/hipo.22500
14. Jensen JH, Helpert JA, Ramani A, Lu H, Kaczynski K. Diffusional kurtosis imaging: the quantification of non-Gaussian water diffusion by means of magnetic resonance imaging. *Magn Reson Med*. 2005;53(6):1432–1440. doi:10.1002/mrm.20508
15. Jensen JH, Helpert JA. MRI quantification of non-Gaussian water diffusion by kurtosis analysis. *NMR Biomed*. 2010;23(7):698–710. doi:10.1002/nbm.1518
16. Liu D, Li K, Ma X, et al. Correlations between the microstructural changes of the medial temporal cortex and mild cognitive impairment in patients with cerebral Small Vascular Disease (cSVD): a diffusion kurtosis imaging study. *Front Neurol*. 2020;11:10. doi:10.3389/fneur.2020.00010
17. Liu H, Liu D, Li K, et al. Microstructural changes in the cingulate gyrus of patients with mild cognitive impairment induced by cerebral small vessel disease. *Neurol Res*. 2021;43:1–9.
18. Patti J, Helenius J, Puri AS, Henninger N. White matter hyperintensity-adjusted critical infarct thresholds to predict a favorable 90-day outcome. *Stroke*. 2016;47(10):2526–2533. doi:10.1161/STROKEAHA.116.013982
19. Zimmerman M, Martinez JH, Young D, Chelminski I, Dalrymple K. Severity classification on the Hamilton depression rating scale. *J Affect Disord*. 2013;150(2):384–388. doi:10.1016/j.jad.2013.04.028
20. Muir RT, Lam B, Honjo K, et al. Trail making test elucidates neural substrates of specific poststroke executive dysfunctions. *Stroke*. 2015;46(10):2755–2761. doi:10.1161/STROKEAHA.115.009936
21. Quinn T, Dawson J, Walters M, Lees K. Functional outcome measures in contemporary stroke trials. *Int J Stroke*. 2009;4(3):200–205. doi:10.1111/j.1747-4949.2009.00271.x
22. Jenkinson M, Beckmann CF, Behrens TE, Woolrich MW, Smith SM. Fsl. *Neuroimage*. 2012;62(2):782–790. doi:10.1016/j.neuroimage.2011.09.015
23. Tabesh A, Jensen JH, Ardekani BA, Helpert JA. Estimation of tensors and tensor-derived measures in diffusional kurtosis imaging. *Magn Reson Med*. 2011;65(3):823–836. doi:10.1002/mrm.22655
24. Smith SM, Jenkinson M, Johansen-Berg H, et al. Tract-based spatial statistics: voxelwise analysis of multi-subject diffusion data. *Neuroimage*. 2006;31(4):1487–1505. doi:10.1016/j.neuroimage.2006.02.024
25. Wakana S, Jiang H, Nagae-Poetscher L, van Zijl P, Mori S. Fiber tract-based atlas of human white matter anatomy. *Radiology*. 2004;230(1):77–87. doi:10.1148/radiol.2301021640
26. Zhao H, Cheng J, Jiang J, et al. Geometric microstructural damage of white matter with functional compensation in post-stroke. *Neuropsychologia*. 2021;160:107980. doi:10.1016/j.neuropsychologia.2021.107980
27. Thong JY, Du J, Ratnarajah N, et al. Abnormalities of cortical thickness, subcortical shapes, and white matter integrity in subcortical vascular cognitive impairment. *Hum Brain Mapp*. 2014;35(5):2320–2332. doi:10.1002/hbm.22330
28. Bubb EJ, Metzler-Baddeley C, Aggleton JP. The cingulum bundle: anatomy, function, and dysfunction. *Neurosci Biobehav Rev*. 2018;92:104–127. doi:10.1016/j.neubiorev.2018.05.008
29. Koshiyama D, Fukunaga M, Okada N, et al. Association between the superior longitudinal fasciculus and perceptual organization and working memory: a diffusion tensor imaging study. *Neurosci Lett*. 2020;738:135349. doi:10.1016/j.neulet.2020.135349
30. Perry ME, McDonald CR, Hagler DJ Jr., et al. White matter tracts associated with set-shifting in healthy aging. *Neuropsychologia*. 2009;47(13):2835–2842. doi:10.1016/j.neuropsychologia.2009.06.008
31. Tuladhar A, van Norden A, de Laat K, et al. White matter integrity in small vessel disease is related to cognition. *NeuroImage Clin*. 2015;7:518–524. doi:10.1016/j.nicl.2015.02.003
32. De Leon Reyes NS, Bragg-Gonzalo L, Nieto M. Development and plasticity of the corpus callosum. *Development*. 2020;147(18). doi:10.1242/dev.189738
33. Zhao L, Wong A, Luo Y, et al. The additional contribution of white matter hyperintensity location to post-stroke cognitive impairment: insights from a multiple-lesion symptom mapping study. *Front Neurosci*. 2018;12:290. doi:10.3389/fnins.2018.00290
34. Roland JL, Snyder AZ, Hacker CD, et al. On the role of the corpus callosum in interhemispheric functional connectivity in humans. *Proc Natl Acad Sci U S A*. 2017;114(50):13278–13283. doi:10.1073/pnas.1707050114
35. Yuan P, Raz N. Prefrontal cortex and executive functions in healthy adults: a meta-analysis of structural neuroimaging studies. *Neurosci Biobehav Rev*. 2014;42:180–192. doi:10.1016/j.neubiorev.2014.02.005
36. Olivo G, Wiemerslage L, Swenne I, et al. Correction: limbic-thalamo-cortical projections and reward-related circuitry integrity affects eating behavior: a longitudinal DTI study in adolescents with restrictive eating disorders. *PLoS One*. 2017;12(4):e0176646. doi:10.1371/journal.pone.0176646
37. Wang Y, Jiang Y, Suo C, et al. Deep/mixed cerebral microbleeds are associated with cognitive dysfunction through thalamocortical connectivity disruption: the Taizhou imaging study. *Neuroimage Clin*. 2019;22:101749. doi:10.1016/j.nicl.2019.101749
38. Zhou N, Masterson SP, Damron JK, Guido W, Bickford ME. The mouse pulvinar nucleus links the lateral extrastriate cortex, striatum, and amygdala. *J Neurosci*. 2018;38(2):347–362. doi:10.1523/JNEUROSCI.1279-17.2017

39. Chou XL, Fang Q, Yan L, et al. Contextual and cross-modality modulation of auditory cortical processing through pulvinar mediated suppression. *Elife*. 2020;9:e54157.
40. Fang Q, Chou XL, Peng B, Zhong W, Zhang LI, Tao HW. A differential circuit via retino-colliculo-pulvinar pathway enhances feature selectivity in visual cortex through surround suppression. *Neuron*. 2020;105(2):355–369 e356. doi:10.1016/j.neuron.2019.10.027
41. Ibrahim LA, Mesik L, Ji XY, et al. Cross-modality sharpening of visual cortical processing through layer-1-mediated inhibition and disinhibition. *Neuron*. 2016;89(5):1031–1045. doi:10.1016/j.neuron.2016.01.027
42. Keser Z, Meier EL, Stockbridge MD, Breining BL, Sebastian R, Hillis AE. Thalamic nuclei and thalamocortical pathways after left hemispheric stroke and their association with picture naming. *Brain Connect*. 2021;11(7):553–565. doi:10.1089/brain.2020.0831
43. Nanda P, Banks GP, Pathak YJ, Sheth SA. Connectivity-based parcellation of the anterior limb of the internal capsule. *Hum Brain Mapp*. 2017;38(12):6107–6117. doi:10.1002/hbm.23815
44. Cheung MM, Hui ES, Chan KC, Helpert JA, Qi L, Wu EX. Does diffusion kurtosis imaging lead to better neural tissue characterization? A rodent brain maturation study. *Neuroimage*. 2009;45(2):386–392. doi:10.1016/j.neuroimage.2008.12.018
45. Steven AJ, Zhuo J, Melhem ER. Diffusion kurtosis imaging: an emerging technique for evaluating the microstructural environment of the brain. *AJR Am J Roentgenol*. 2014;202(1):W26–33. doi:10.2214/AJR.13.11365
46. Nakajima R, Kinoshita M, Shinohara H, Nakada M. The superior longitudinal fascicle: reconsidering the fronto-parietal neural network based on anatomy and function. *Brain Imaging Behav*. 2020;14(6):2817–2830. doi:10.1007/s11682-019-00187-4
47. Lee CY, Bennett KM, Debbs JP. Sensitivities of statistical distribution model and diffusion kurtosis model in varying microstructural environments: a Monte Carlo study. *J Magn Reson*. 2013;230:19–26. doi:10.1016/j.jmr.2013.01.014

Neuropsychiatric Disease and Treatment

Dovepress

Publish your work in this journal

Neuropsychiatric Disease and Treatment is an international, peer-reviewed journal of clinical therapeutics and pharmacology focusing on concise rapid reporting of clinical or pre-clinical studies on a range of neuropsychiatric and neurological disorders. This journal is indexed on PubMed Central, the 'PsycINFO' database and CAS, and is the official journal of The International Neuropsychiatric Association (INA). The manuscript management system is completely online and includes a very quick and fair peer-review system, which is all easy to use. Visit <http://www.dovepress.com/testimonials.php> to read real quotes from published authors.

Submit your manuscript here: <https://www.dovepress.com/neuropsychiatric-disease-and-treatment-journal>